PLANAR CRACK ASSUMPTION AS AN ALTERNATIVE TO NAVIER'S HYPOTHESIS IN THE MODELLING OF FIBER-REINFORCED CONCRETE SECTIONS

JACINTO R. CARMONA[*†], JUAN REY-REY[†], GONZALO RUIZ[††] AND JUAN M. RODRÍGUEZ-MADUEÑO[††]

[†]Universidad Politécnica de Madrid (UPM)
Madrid, España
[*]e-mail: jacinto.ruiz@upm.es
e-mail: juan.rey@upm.es

[††]Universidad de Castilla-La Mancha (UCLM)
Ciudad Real, España
e-mail:gonzalo.ruiz@uclm.es

Key words: Cohesive fracture, Fiber Reinforced Concrete, Size effect

Abstract: The present article describes a model, based on concepts of Fracture Mechanics, to evaluate the behavior of fiber reinforced concrete (FRC) sections. It is developed by an analytical method that represents tension in concrete by means of the linear softening law (σ-w) included in the Model Code 2010. The method also uses a compatibility equation for the cracked zone based on the planar crack hypothesis, i.e. the assumption that the crack surfaces remain plane throughout the fracture process, in conjunction with the Navier's hypothesis applied only to the non-cracked zone. The model reproduces the experimental size-effect on the rupture-modulus for concrete and FRC sections and points at Hillerborg's brittleness number as a common characterization parameter for concrete and FRC sections behavior. The study concludes that planar crack assumption can be considered as an alternative to Navier's hypothesis, since it gives a more physical approximation to the FRC fracture behavior.

1 INTRODUCTION

Fiber Reinforced Concrete (FRC) behavior, when it is considering post-cracking softening, is generally modelled by a stress-strain law (σ-ε) related to a stress-crack opening law (σ-w). This stress-crack opening law represents tension uniaxial fiber reinforced concrete behavior. To connect continuous mechanics, governed by a stress-strain constitutive relationship, and fracture mechanics, governed by a stress-crack, a parameter namely the structural characteristic length (lcs) of the structural element is defined [1, 2]. The evaluation of this parameter is not clear in the bibliography and introduces the idea that concrete is a continuous material, when in fact the main consequence of concrete softening is the crack localization, which introduces a discontinuity in the material.

On the other hand, when dealing with finite element models (FEMs), it is necessary to introduce a specific internal length (Li), which depends on the cracking model implemented in the program. Hence, the afore mentioned

internal length is not a structural material property but it represents a "numerical parameter" for bridging in another easy way, the continuous mechanics to the fracture one. In order to properly perform this connection and to prevent mesh dependency, several methods have related the internal length to physical parameters, such as maximum aggregate size for non-local approaches [3-5], or to element size for local approaches [6, 7].In addition, several numerical discontinuous crack models have been developed. Among them, it can be cited that discontinuous numerical modeling of fracture using embedded discontinuities [8], discrete strong discontinuity approach [9], dynamic fragmentation [10] and the sequentially linear analysis method [11].

In the case of analytical models to describe flexural behavior of FRC sections, the use of a continuous stress-strain constitutive law, is always linked together with the use of Navier's hypothesis, as compatibility equation (planar section remains planar after deformation) [12]. This methodology doesn`t represent the concrete behavior properly as concrete is considered as a continuous material and the physical phenomenon of cracking is not properly described [13].

In order to avoid the use of length parameters as *lcs* to represent fiber reinforced behavior, in this work is presented a model, based on concepts of Fracture Mechanics, to evaluate the flexural behavior of fiber reinforced concrete sections. It is developed by an analytical method that represents tension in concrete by means of the linear stress-crack opening law (σ-w) included in Model Code 2010 [2]. The method also uses a compatibility equation based on the planar crack hypothesis, i.e. the assumption that the crack surfaces remain plane throughout the fracture process, which has been recently proven true by means of digital image correlation [14]. The compressive behavior of FRC is modeled through a linear elastic law (σ-ε) in conjunction with the Navier's hypothesis, applied only to the ligament. Crack opening is evaluated from the applied moment and the crack depth, in the same way that it was proposed in references [15-16], using an expression proposed by Tada et al. [17].

The paper is structured as follows. The subsequent section describes the material constitutive assumptions made. Section 3 describes the crack propagation theoretical model developed. A discussion on the model response and size effect is included in Section 4. Finally, Section 5 summarizes the results of the paper and draws several conclusions.

2 MATERIAL HYPOTHESIS

Fiber Reinforced Concrete (FRC) behavior is divided in two different cases depending on the development of the fracture process. It is considered one hypothesis for the non-cracked zone and other for the cracked zone.

2.1 Non-cracked zone

In the non-cracked area, concrete behavior is considered as an elastic material, which is represented by its elastic modulus. Navier´s hypothesis is used as compatibility equation in the non-cracked area, see Fig. 1.

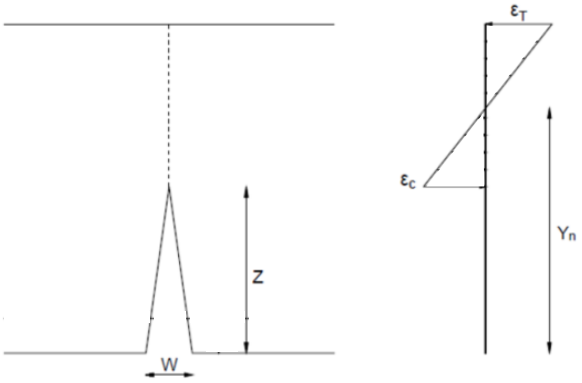

Figure 1: Material hypothesis. Cracked area is modelled according to the crack planar hypothesis and non-cracked area according to Navier's hypothesis.

2.2 Cracked zone

Based on the cohesive model, a stress-crack opening law in uniaxial tension is defined as constitutive law for representing the post-cracking behaviour of FRC, as is defined in

Model Code 2010 [2].A softening linear post-cracking behaviour is used in the model as shown schematically Fig.2. The model showed in this paper is only valid for the case of post-cracking softening, case where a discrete crack is localized in the Fibre Reinforced Concrete section. Post cracking hardening has to be modelled through plasticity models as no crack localizations will take place.

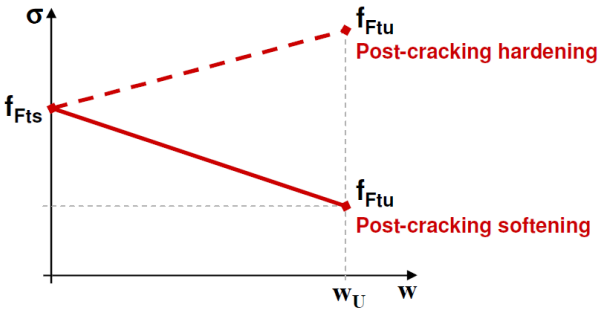

Figure 2: Simplified post-cracking constitutive law: stress-crackopening (softening post-cracking behaviour) [2].

In Fig. 2,f_{Fts} represents the serviceability residual strength, defined as the post-cracking strength for serviceability crack openings, and f_{Ftu} represents the ultimate residual strength.

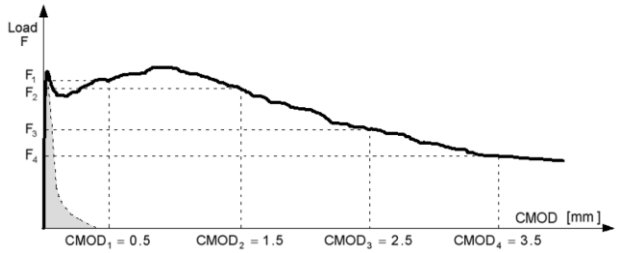

Figure 3: Applied force (F) versus Crack Mouth Opening displacement (CMOD) [2].

f_{Fts} *and* f_{Ftu} have to be calculated through the residual values of flexural strength by using the following equations:

$$f_{Fts} = 0.45 f_{R1} \quad (1)$$

$$f_{Ftu} = f_{Fts} - \frac{w_u}{CMOD_3}(f_{Fts} - 0.5 f_{R3} + 0.2 f_{R1}) \quad (2)$$

Where $f_{R1}$is the residual flexural tensile strength corresponding to *CMOD* = *CMOD1* = 0.5mm and$f_{R3}$is the residual flexural tensile strength corresponding to *CMOD* = *CMOD3* = w_u. These parameters are determined by performing a 3-point bending test, on a notched beam, according to EN 14651, see Fig. 3.w_u usually adopts the value of 2.5mm.

The ultimate tensile strength f_{Ftu} in this linear model depends on the required ductility that is related to the allowed crack width. The ultimatecrack width, in any case, may not exceed 2.5 mm.The crack opening, *w*, in postcracking constitutive lawcan be expressed as:

$$w = \frac{f_{Fts} - \sigma}{f_{Fts} - f_{Ftu}} w_u \quad (3)$$

The area under the softening function represents the Fracture Energy, $G_{F,FRC}$.

$$G_{F,FRC} = \frac{f_{Fts} + f_{Ftu}}{2} w_u \Rightarrow w_u = \frac{2G_{F,FRC}}{f_{Fts} + f_{Ftu}} \quad (4)$$

Planar crack assumption is used as compatibility equation in the non-cracked area. Based on this assumption a linear softening can be considered on the cohesive ligament, see Fig 4.

3 MODELLING OF CRACK PROPAGATION

A rectangular concrete section is considered. The different geometric variables relevant to the problem are displayed in Fig. 4.The section has a depth *h*, and a width equal to *b*. The crack depth is represented as *z* and the neutral axis depth as y_n. All these dimensions can be expressed in a non-dimensional way by dividing themby the depth *h*. In this manner, we define $\xi = z/h$ as the crack depth expressed in a non-dimensional form and $\gamma_n = y/h$ the depth of the neutral axis in a non-dimensional form; these parameters have a value between 0 and 1. Crack opening is expressed in non dimensional form by dividing it by the ultimate crack width, $w^* = w/w_u$.

Crack modelling is divided in two cases depending on the crack opening at the bottom part of the section. Section is considered to be

in case 1, when the crack openings is less than the ultimate crack width, $w_b < w_u$, and it is in case 2 when $w_b > w_u$, See Fig. 4.

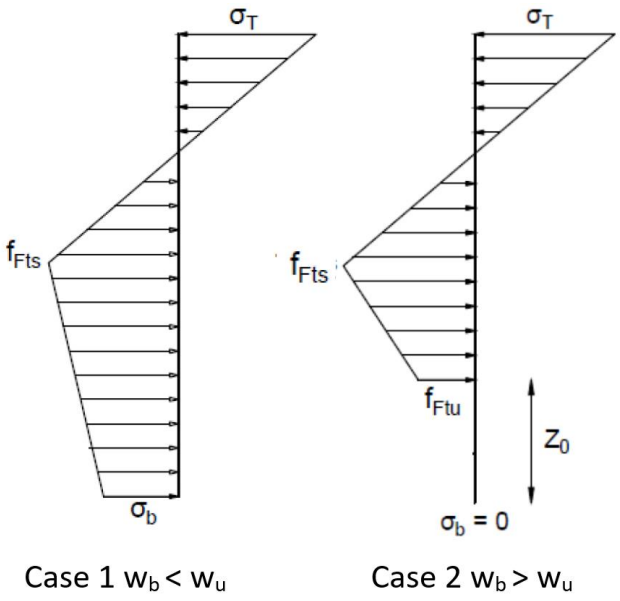

Figure 4: Crack propagation modelling cases.

In case 2, the crack depth for the critical opening is represented as z_0, in non dimensional form is defined as $\xi_0 = z_0/h$.

Stress at the bottom part is represented as σ_b and stress at the top as σ_t. Non dimensional stresses are defined dividing the stress by the serviceability residual strength, f_{Fts}. So, we define $\sigma_b^* = \sigma_b / f_{Fts}$ and $\sigma_t^* = \sigma_t / f_{Fts}$.

3.1 case 1, $w_b < w_u$

The section equilibrium forces can be expressed as:

$$\sum \mathrm{F} = 0 \implies \frac{\sigma_T}{2}(h - y_n)b - \frac{f_{Fts}}{2}(y_n - z)b + \left(\frac{f_{Fts}+\sigma_b}{2}\right) * zb \quad (5)$$

Expressing Eq. (5) in a non-dimensional form the following is obtained:

$$\sigma_t^* = \frac{\gamma_n + \sigma_b^* \xi}{1-\gamma_n} \quad (6)$$

Compatibility condition in non-cracked zone is represented based on Navier´s hypothesis:

$$\frac{\varepsilon_T}{h-y_n} = \frac{\varepsilon_{ct}}{y_n - z} \Rightarrow \frac{\sigma_T}{h-y_n} = \frac{f_{Fts}}{y_n - z} \quad (7)$$

Expressing Eq. (3) in a non-dimensional form the following equation is obtained:

$$\gamma_n = \frac{1+\sigma_T^* \xi}{1+\sigma_T^*} \quad (8)$$

In the cracked zone, constitutive law is formulated as:

$$w_b(M,z) = w_b(\sigma_b) \quad (9)$$

Crack opening, $w_b(M,z)$ can be evaluated by the expression given by Tada et al [17]. $w_b(\sigma_b)$ is defined considering the softening law, Eq. (3). Thus, Eq. (9) can be expressed as:

$$\frac{24M}{bh^2 E_c} z f(\xi) = \frac{f_{Fts} - \sigma_b}{f_{Fts} - f_{Ftu}} \quad (10)$$

Where f(ξ) is a shape function:

$$f(\xi) = 0.76 - 2.28\xi + 3.87\xi^2 - 2.04\xi^3 + \frac{0.66}{(1-\xi)^2} \quad (11)$$

If we define a characteristic length as:

$$l_{ch,FR} = \frac{E_c G_{F,FR}}{f_{Fts}^2 - f_{Ftu}^2} \quad (12)$$

A brittleness numbercan be defined as:

$$\beta_{H,FR} = \frac{h}{l_{ch,FR}} \quad (13)$$

This brittleness number can be considered a generalization of the Hillerborg's brittleness number [12] for the case of linear softening shown in Fig. 2. Thus,Eq. (10) in non-dimensional form is expressed as:

$$\sigma_b^* = 1 - 12 M^* \beta_{H,FR} \xi f(\xi) \quad (10)$$

Where M^* is the bending moment in the

section expressed in non-dimensional form

$$M^* = \frac{M}{bh^2 f_{Fts}} \quad (11)$$

Bending moment in the section is equal to:

$$M = \frac{1}{3}\sigma_t (h - y_n)^2 b + . f_{FTs}\,(y_n - z)^2 b + \left(\frac{f_{FTs} + \sigma_b}{2}\right) z\left(y_n - z\left(\frac{\frac{1}{3}f_{FTs} + \frac{1}{6}\sigma_b}{\frac{1}{2}(f_{FTs} + \sigma_b)}\right)\right) b \quad (12)$$

Writing Eq. (12) in a non-dimensional form itis obtained that:

$$M^* = \frac{1}{3}\sigma_t^* (1 - \gamma_n)^2 + \frac{1}{3}(1 - \xi)^2 + \left(\frac{1 + \sigma_b^*}{2}\right)\xi\left(\gamma_n - \xi\left(\frac{2 + \sigma_b^*}{3(1 + \sigma_b^*)}\right)\right) \quad (13)$$

In order to evaluate the section stress profile,crack opening and bending moment for a given crack depth, ξ,a system of four equations, Eqs. (6), (8), (10) and (13), has to be solved analytically. The results of the equation system are σ^*_T, σ^*_T, $\gamma_n$and M^*, the only input data is$\beta_{H,FR}$. Crack depth,ξ, is used as control parameter during de crack process. For each crack depth, only one equilibrium solution exists.

Crack opening at bottom part of the sectionis evaluated as:

$$w_b^* = 12M^* \beta_{H,FRC}\,\xi f(\xi)\left(\frac{1}{1 - \alpha}\right) \quad (14)$$

Where α is defined as the ratio between f_{Ftu} and f_{Fts}

3.2 case 2, $w_b > w_u$,

We proceed in the same way that in the previous case. The section equilibrium forces can be expressed as:

$$\sum \mathrm{F} = 0 \implies \frac{\sigma_T}{2}(h - y_n)b - \frac{f_{Fts}}{2}(y_n - z)b + \left(\frac{f_{Fts} + f_{Ftu}}{2}\right) * (z - z_0)b \quad (15)$$

Expressing Eq. (5) in a non-dimensional form:

$$\sigma_t^* = \frac{\gamma_n + \alpha\xi + \xi_0(1 + \alpha)}{1 - \gamma_n} \quad (16)$$

In case 2, the equation to represent the compatibility condition in non-cracked zone is the same as for case 1, Eq (7) and (8).

As crack surface is considered that it has a linear variation from 0 to w_b, crack opening for any depth is evaluated multiplying the crack at the bottom, w_b by the term $1\text{-}z/z_0$. So,the compatibility condition at the cracked zone can be formulated as:

$$w_b(M, z)\left(1 - \frac{z}{z_0}\right) = w_u \quad (17)$$

By substituting $w_b(M, z)$ for its value, Eq. (16)can be rewritten as:

$$\frac{24M}{bh^2 E_c} z f(\xi)\left(1 - \frac{z}{z_0}\right) = w_u \quad (18)$$

Eq. (17) in non-dimensional form is expressed as:

$$\xi_0 = \xi - \frac{1 - \alpha}{12M^* \beta_{H,FR} f(\xi)} \quad (19)$$

Finally,bending moment in case 2 in the section is equal to:

$$M = \frac{1}{3}\sigma_t (h - y_n)^2 b + \frac{1}{3} f_{FTs}\,(y_n - z)^2 b + f_{FTu}(z - z_0)\left(y_n - z + \frac{z - z_0}{2}\right) b + \frac{1}{2}\,(f_{FTs} - f_{FTu})(z - z_0)\left(\frac{1}{3}(z - z_0) + y_n - z\right) b \quad (20)$$

Expressing Eq. (19) in a non-dimensional form:

$$M^* = \frac{1}{3}\sigma_t^* (1 - \gamma_n)^2 + \frac{1}{3}(1 - \xi)^2 + \alpha(\xi - \xi_0)\left(\gamma_n - \frac{1}{2}\left(\frac{\xi + \xi_0}{2}\right)\right) + \frac{1}{2}\,(1 - \alpha)(\xi - \xi_0)\left(\gamma_n - \frac{1}{3}(2\xi + \xi_0)\right) \quad (21)$$

To evaluate the section stress profile crack in case 2, depth for critical crack opening and bending moment for a given crack depth, ξ, a system of three equations, Eqs. (16), (8), (19) and (21), can be solved analytically. From the system are evaluated σ^*_T, ξ_0, γ_n and M^*, the input data are $\beta_{H,FR}$ .and α.Crack opening is evaluated through the following expression:

$$w_b^* = \frac{\xi}{\xi - \xi_0} \qquad (22)$$

4. RESULTS AND DISCUSSION

4.1 Model response

In this section it will be shown how the value of the $\beta_{H,FRC}$ affects the behavior of the section. In Fig. 4a the x-axis represents the non-dimensional crack opening, w*, and the y-axis the non dimensional bending moment during crack growth, *M**.

The ratio between f_{Fts} *and* f_{Ftu}, α, has a value of 0.8.Cracking moment, if we consider an elastic material, has a non dimensional value of 0.167, and all curves has this value as initial point. As the brittleness number decreases, peak load increases. When it reaches a value of the non imensional crack opening of 1, a decreasing in the bending moment occurs. This decreasing is bigger for sections whose value of $\beta_{H,FRC}$ its smaller.

In Fig. 4b the x-axis represents the non-dimensional crack depth, ξ, and the y-axis the non dimensional bending moment during crack growth, *M**. It shows the same results that in Fig. 4a. In this case, it is observed that peak load is reached for a bigger value of the crack depth as the value of $\beta_{H,FRC}$ is smaller. Thus for smaller values of $\beta_{H,FRC}$ the softening length development in the fiber reinforced concrete section is bigger, and that is the main reason for the peak load increases.

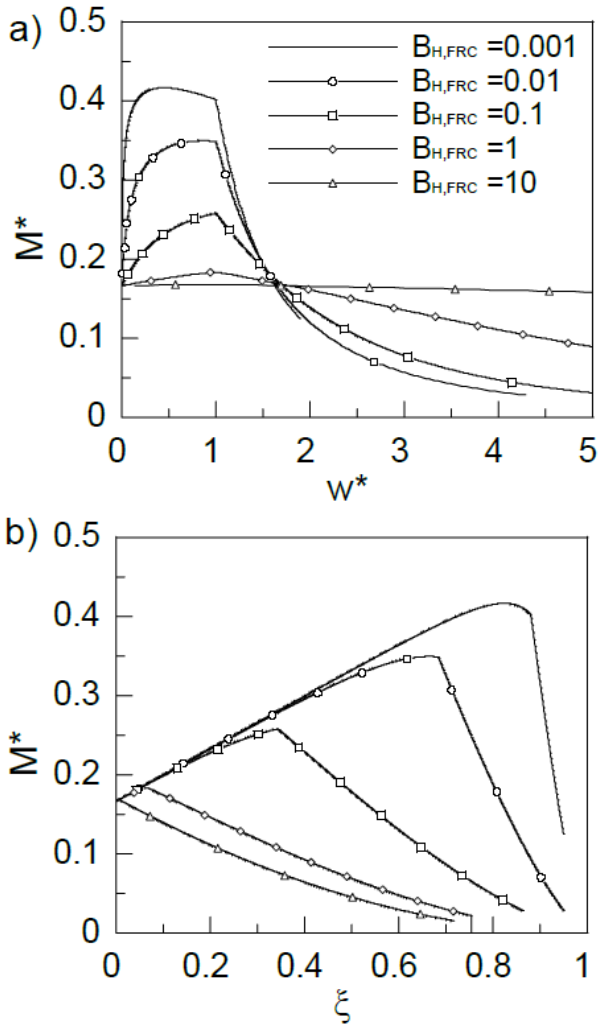

Figure 4: influence of $\beta_{H,FRC}$: a) M*-w* curves; b) M*-ξ curves.

Fig. 5a shows the influence of the ratio between f_{Fts} *and* f_{Ftu}, α, in the fibre reinforced concrete behaviour.As in the previous case, the x-axis represents the non-dimensional crack opening, *w**, and the y-axis represents the non dimensional bending moment duringcrack growth, *M**.$\beta_{H,FRC}$, has a constant value of 0.01 in the results showed.

As the value of the ratio α increases the bending moment, for a given crack opening, increases. Peak load is not influenced by this parameter as clearly it is showed in Fig. 5b, where a detail of Fig 5a is zoomed. In all cases we concluded that peak load occurs when the crack opening is less or equal to the value of w_u.

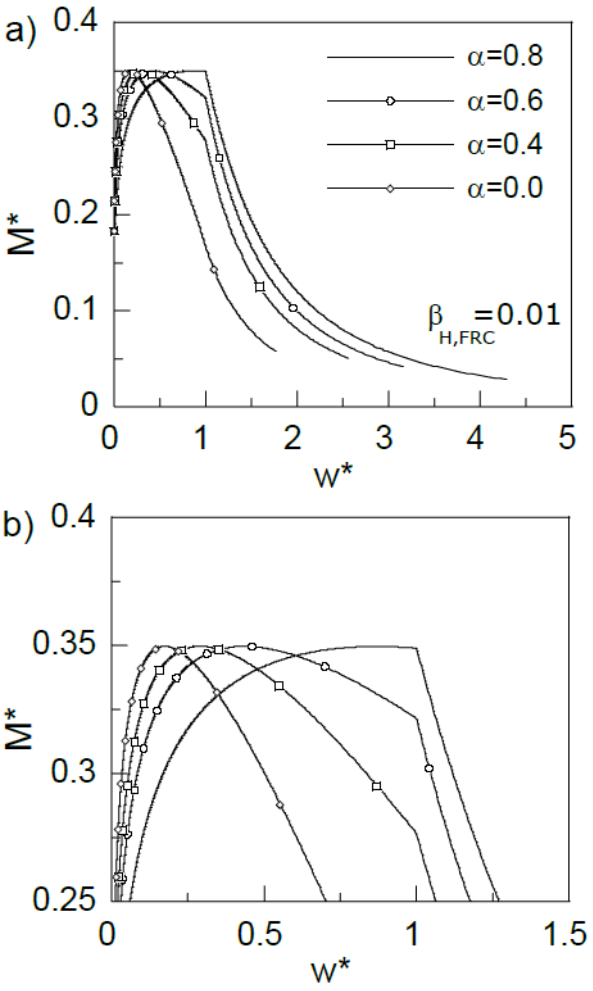

Figure 5: Influence of α: a) M*-w* curves; b) M*-w* detail.

4.2 Comparison between model response and experimental results

To validate the response of the model, we have compared theresults obtained with those obtained by a recent experimental program performed by Carpinteri at al. [18]. A total of nine geometricallysimilar beams reinforced with 3 different fiber volume ratios were tested, 10 , 20 and 40 fiber kg/m3 of concrete (3 beams for each ratio). In this experimental program, all concrete properties were determined from independent tests.

Fiber (kg/m)	*h (mm)*	*B (mm)*	*L (mm)*	f_{Fts}(MPa)	f_{Ftu}(MPa)
10	200	100	1200	2.36	0.42
20	200	100	1200	1.39	0.16
40	200	100	1200	3.21	1.42

Table 1: Beams characteristics [18].

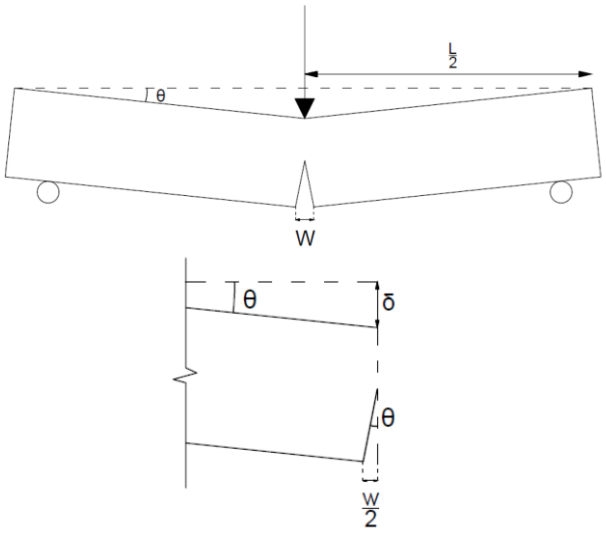

Figure 6: Displacement evaluation

In order to compare test results with the model, some hypothesis have been done.If we consider that the vertical displacement is provoked by the crack opening, see Fig.. 6, and elastic deformation is neglected, the vertical displacement can be evaluated through the crack depth and crack opening.

Section rotation is equal to:

$$\theta \cong \frac{w/_2}{z} = \frac{w^*/_2}{\xi}\frac{w_u}{h} \qquad (22)$$

Thus, beam deflection at midpoint can be evaluated as:

$$\delta = \theta\frac{L}{2} = \frac{w^*/_2}{\xi}\frac{w_u}{h}\frac{L}{2} \qquad (23)$$

Load applied is evaluated from the bending moment of crack propagation by the relation:

$$P = \frac{4M}{L}\ where\ M = M^* b h^2 f_{Fts} \qquad (24)$$

Fig. 7 shows a comparison between experimental and model results. The x-axis represents vertical displacement under the point load, δ, and the y-axis represents the applied load, P.

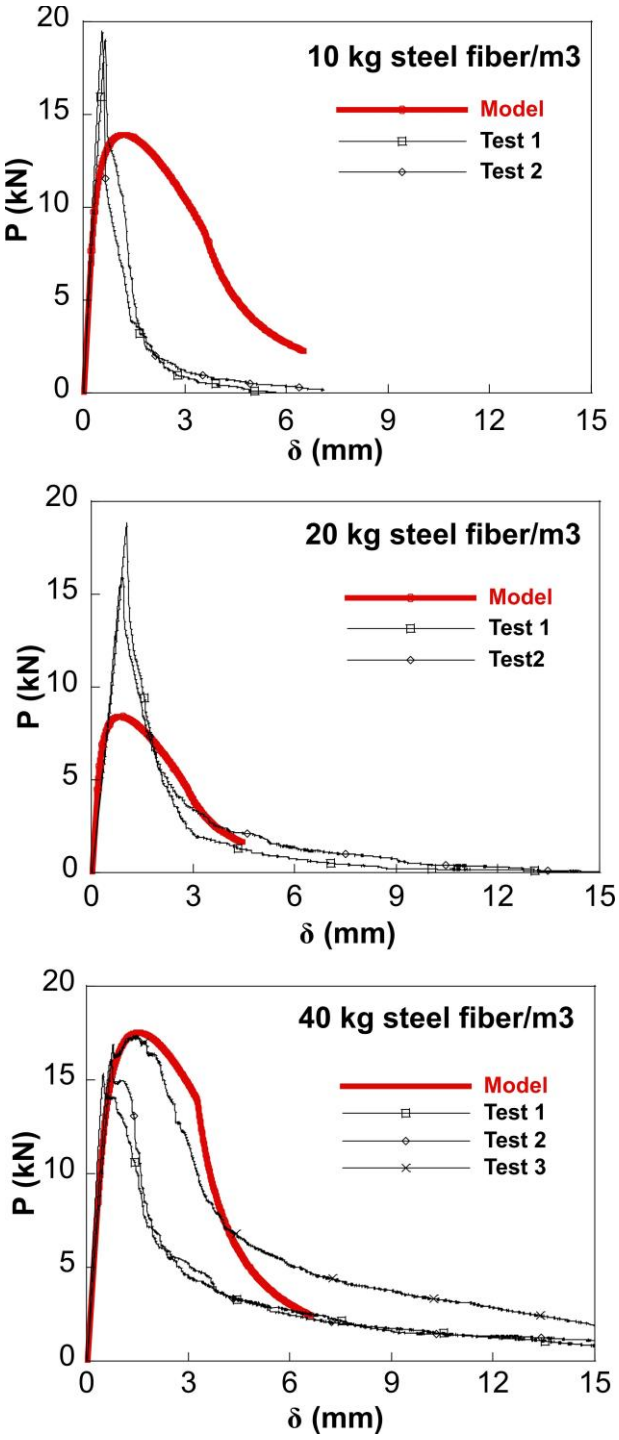

Figure 7: Experimental - model results comparison.

For the lowest fiber ratio, model response does not fit correctly the tests results. As fiber quantityincreases, the curves given by the model fit the experimental results better.

The model follows the experimental trends in FRC sections, although it shows some limitations stemming from the use of the linear softening law in Model Code 2010. This softening law represents correctly the residual behaviour as is shown in comparison for 20 and 40 kg of steel fibre per m^3 of concrete. For low fibre quantities peak load is controlled by tension concrete strength, as is shown in Fig.8 and linear softening law in Model Code 2010 does not represent correctly the initial curveshape.

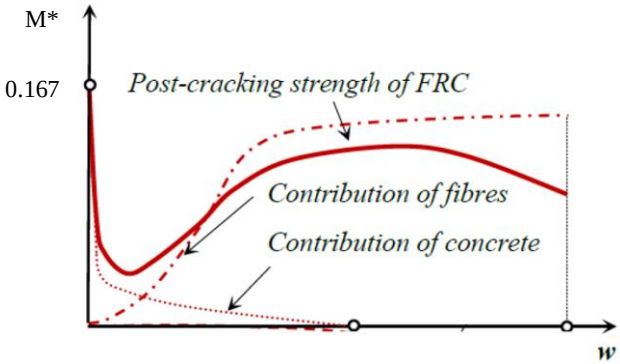

Figure 8: Scheme of contribution of concrete and fibres to FRC response [19].

4.3 Size effect on the modulus of rupture for FRC

The modulus of rupture provides a measure of the strength of plain and fibre reinforced concrete. The modulus of rupture is defined as:

$$f_r = \frac{6M_{peak}}{bh^2} \qquad (25)$$

Where $M_{peak}$is the maximum bending moment in the curve M-w. The modulus of rupture was originally assumed as a material property coinciding with the tensile strength but results from cohesive models showed that rupture modulus was size-dependent and also dependent on the softening curve [13].

In the proposedmodel, linear concrete softening can be represented when α=0. Thus the expressions derived at section 3 are valid for plain concrete and FRC. On the other hand, the peak load occurs always during case 1. The input data from the model is only the brittleness number $\beta_{H,FRC,}$ which can be considered as an intrinsic size on the FRC

element. The dependency of size effectof a brittleness number is proved in references [20-22].

In Fig. 9a the x-axis represents the brittleness number,$\beta_{H,FRC}$, and the y-axis represents the non dimensional rupture modulus, σ^*_R, which is defined as the ratio between the peak load,f_r, and f_{Fts}(initial concrete or FRC tension strength in the linear softening curve).

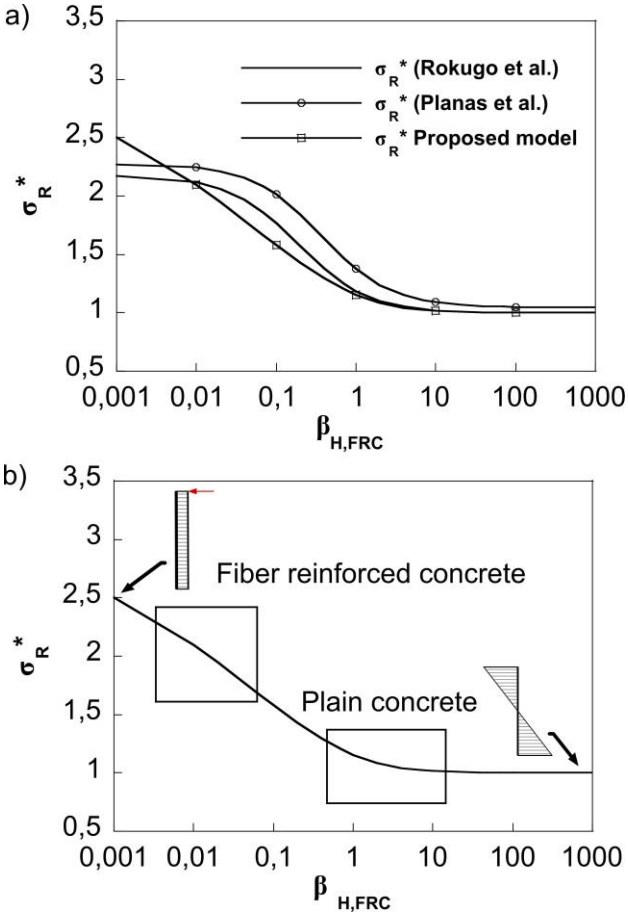

Figure 9: Size effect (a) dependent of rupture modulus on $\beta_{H,FRC}$. (b)asymptotic behavior.

The figures show the size effect dependency of the rupture modulus evaluated by the expressions given by Rokugo at al. [21] and Planas at al. [22]. The results obtained by the model proposed in this paper are also drawn.

Theproposed model is approximately valid for the entire range of sizes, satisfying the condition that $\sigma^*_R \rightarrow 3$ for $\beta_{H,FRC} = 0$ (plastic limit solution for cohesive cracks) and $\sigma^*_R \rightarrow 1$for $\beta_{H,FRC} = \infty$, as is showed in Fig 9b (elastic solution).

Although the proposed model fits the trend on the size effect, some improvement in the shape function $f(\xi)$can be done to fit better the results proposed in references [21-22].

Finally, Fig. 9b shows the curve zones located mostly on structural members designed by plain concrete or FRC. It is observed that influence of size effect is stronger for FRC elements than for plain concrete elements. In all cases the model identifies the plain concrete and FRC in the same theoretical frame which can help to understand better behavior of FRC elements.

5 CONCLUSIONS

A model based on Concrete Fracture Mechanicsis presented. The model reproduces the experimental size-effect on the rupture-modulus for concrete and FRC sections. It also points a brittleness number based on Hillerborg's brittleness number as a common characterization parameter for concrete and FRC sections behaviour. The model follows the experimental trends in FRC sections, although it shows some limitations stemming from the use of the linear softening law in Model Code 2010. Based on the results, a design method is proposed which uses diagrams that represent bending moment capacity against crack opening (M-w curves).

The study concludes that planar crack assumption can be considered as an alternative to Navier's hypothesis, since it gives a more physical approximation to the FRC fracture behavior. It is also concluded that linear softening law in Model Code 2010 represents FRC residual behavior for medium and high fiber contentsbut does not represent correctly FRC behavior for low fiber contents. Finally, it is showed that influence of size effect is stronger for FRC elements than for plain concrete elements.

ACKNOWLEDGEMENT

Jacinto R. Carmona acknowledged the financial support given by the *Ministerio de Ciencia Innovación y Universidades* through grant PTQ-15-07633 to support his research activity.

REFERENCES

[1] Di Prisco M., Colombo M., Dozio D., 2013. Fibre-reinforced concrete in fib Model Code 2010: principles, models and test validation, *Structural Concrete*, Vol. 14, No.4

[2] *Fib Model Code for Concrete Structures 2010* (2012), Final Complete Draft, fib bulletins 65 and 66, March 2012-ISBN 978-2-88394-105-2 and April 2012-ISBN 978-2-88394-106-9.

[3] Bazant, Z. P., Cedolin, L., 1983. Finite element modelling of crack band propagation, *Journal of Structural Engineering* 109(1), 1983, pp.69-92.

[4] Bazant, Z. P., 1994. Nonlocal damage theory based on micromechanics of crack interactions, *Journal of Engineering Mechanics*, ASCE, 120(3), pp.593-617, 1401-1402

[5] Ferrara, L., di Prisco, M., 2001. Mode I fracture behaviour in concrete: non-local damage modelling, ASCE, *Journal of Engineering Mechanics*, 127(7), 2001, pp.678-692.

[6] Cervenka, V., Pukl R., 1995. Mesh sensitivity effects in smeared finite element analysis of concrete fracture, *inProceedings of FramCoS 2*, pp.1387-1396

[7] Belletti, B., Hendriks, M.A.N., Rots, J.G., 2008. Finite element modelling of FRC structures – pitfalls and how toavoide them. *In: Proceedings of BEFIB 2008*, pp. 303-313.

[8] Alfaiate, J., Wells, G.N., Sluys, L.J., 2002. On the use of embedded discontinuity elements with crack path continuityfor mode-I and mixed-mode fracture. *Engineering Fracture Mechanics*, 69 (6), pp. 661-686.

[9] Dias-da-Costa, D., Alfaiate, J., Sluys, L.J., Júlio, E., 2009. A discrete strong discontinuity approach. *Engineering Fracture Mechanics*, 76 (9), pp. 1176-1201.

[10] Yu, R.C. and Ruiz, G., 2006. Explicit finite element modeling of static crack propagation in reinforced concrete. *International Journal of. Fracture*.141:357-72.

[11] Hendriks, M.A.N., Rots, J.G., 2013. Sequentially linear versus nonlinear analysis of RC structures, 2013, *Engineering Computations* (Swansea, Wales), 30 (6), pp. 792-801

[12] Barros,J. A. and Figueiras J. A., 1999. Flexural behaviour of SFRC: testing and modelling. *Journal of materials in civil engineering*, vol. 11, no. 4, pp. 331-339, 1999.

[13] Bažant Z.P. andPlanas J., 1998. *Fracture and size effect in concrete and other quasibrittle materials*. Boca Raton: CRC Press.

[14] Gali,S. and, Subramaniam,K.V.L., 2017. Multi-linear stress-crack separation relationship for steel fiber reinforced concrete: Analytical framework and experimental evaluation, *Theor. Appl. Fract. Mech.* (2017), http://dx.doi.org/10.1016/j.tafmec.2017.06.018

[15] Carmona, J. R. and Ruiz, G., 2014. Bond and size effects on the shear capacity of RC beams without stirrups. *Engineering Structures*, vol. 66, pp. 45-56.

[16] Carmona, J. R. and López G. R., 2017.

Modelo analítico para el análisis de la flexión y la fisuración en secciones de hormigón armado como alternativa al diagrama de pivotes. *Hormigón y Acero*, vol. 68, no. 282, pp. 147-154.

[17] Tada, H., Paris, H. and Irwin, G., 1973. *The stress analysis of cracks handbook*. Del ResearchCorporation.

[18] Carpinteri,A., Cadamuro E., and Ventura G., 2015. Fibre-reinforced concrete in flexure: a cohesive/overlapping crack model application.*Materials and Structures*, vol. 48,no. 1-2, pp. 235-247, 2015.

[19] Li VC, Stang H, Krenchel H., 1993. Micromechanics of crack bridging in fiber reinforced concrete, *Materials and Structures*, 26(162):486-494.

[20] Bažant Z.P., 1987. Fracture energy of heterogeneous materials and similitude. In preprints SEM-RILEM *IntConf on Fracture of Concrete and Rocks. Society for experimental Mechanics* (SEM), Bethel pp 390-402, *Materials and Structures*, 26(162):486-494.

[21] Uchida, Y. Rokugo, K. and Konayagi, W., 1992. Application of fracture mechanics to size effect on flexural strength of concrete. *In Proceedings of JSCE Concrete engineering and pavements* (442) 101-107.

[22] Planas, J., Guinea, G. and Elices, M,. 1995. Rupture modulus and fracture properties of concrete. *In FRAMCOS* Vol 1 F.H. Wittmann ed. Aedificatio Publishers Freiburg Germany pp 95-110.